Glio- and neuroprotection by prosaposin is mediated by orphan G-protein coupled receptors GPR37L1 and GPR37

Journal:	*GLIA*
Manuscript ID	GLIA-00070-2018.R1
Wiley - Manuscript type:	Original Research Article
Date Submitted by the Author:	n/a
Complete List of Authors:	Liu, Beihui; University of Bristol Mosienko, Valentina; University of Bristol, Physiology, Pharmacology and Neuroscience Vaccari Cordoso, Barbara; University of Bristol, Physiology, Pharmacology and Neuroscience Prokudina, Daria; Immanuel Kant Baltic Federal University, University of Bristol Huentelman, Mathew; Translational Genomics Research Institute (TGen), 445 N Fifth Street, Phoenix, AZ 85004, USA Teschemacher, Anja; University of Bristol, Physiology, Pharmacology and Neuroscience Kasparov, Sergey; University of Bristol, Physiology, Pharmacology and Neuroscience
Key Words:	astrocyte, orphan GPCR, GPR37L1, protection, oxidative stress
Note: The following files were submitted by the author for peer review, but cannot be converted to PDF. You must view these files (e.g. movies) online.	
Suppl movie 1 full media.avi Suppl movie 2 PSAP Depleted Media.avi Suppl movie 3 PSAP Depeleted Media +TX14(A).avi Suppl movie 4 PSAP Depleted Media +TX14(A)+miRNA-KNOCK DOWN.avi Suppl movie 5 PSAP Depleted Media +TX14(A)+ miRNA-negative.avi	

Glio- and neuroprotection by prosaposin is mediated by orphan G-protein coupled receptors GPR37L1 and GPR37

Running title: Neuroprotective receptors on astrocytes

Beihui Liu*, Valentina Mosienko*, Barbara Vaccari Cardoso*, Daria Prokudina**, Mathew Huentelman[#], Anja G. Teschemacher*, Sergey Kasparov*

* - Department of Physiology, Pharmacology and Neuroscience, University of Bristol, Bristol, BS8 1TD, UK

- Translational Genomics Research Institute (TGen), 445 N Fifth Street, Phoenix, AZ 85004, USA

** - Baltic Federal University, Kaliningrad, Russian Federation, 236041

ACNOWLEDGEMENTS

This work was supported by the grants from MRC, MR/L020661/1 and BBSRC, BB/L019396/1. BVC is funded by a Science without Borders scholarship from the BNCTSD (206427/2014-0).

We are grateful to Professor K Jalink (The Netherlands Cancer Institute, Amsterdam, The Netherlands) for the gift of the EPAC sensor. We thank Dr HJ Bailes (University of Manchester, Manchester, UK) for the help with setting up Glosensor assay.

Main points

1.Prosaptide TX14(A), a fragment of Saposin C, acts via GPR37L1/GPR37 on astrocytes and protects them from the oxidative stress.

2. In HEK293 cells GPR37L1 and GPR37 are dysfunctional.

3. GPR37L1/GPR37 signaling in astrocytes enables neuroprotection.

WORDS:

TOTAL: 9572

ABSTRACT: 224

INTRODUCTION: 757

METHODS: 2917

RESULTS: 1254

DISCUSSION: 1414

Correspondence:

S Kasparov or A.G. Teschemacher (joint senior authors)

Sergey.Kasparov@Bristol.ac.uk

Anja.Teschemacher@Bristol.ac.uk

ABSTRACT

Discovery of neuroprotective pathways is one of the major priorities for neuroscience. Astrocytes are the natural neuroprotectors and it is likely that brain resilience can be enhanced by mobilising their protective potential. Among G-protein coupled receptors expressed by astrocytes, two highly related receptors, GPR37L1 and GPR37, are of particular interest. Previous studies suggested that these receptors are activated by a peptide Saposin C and its neuroactive fragments (such as prosaptide TX14), which were demonstrated to be neuroprotective in various animal models by several groups. However, pairing of Saposin C or prosaptides with GPR37L1/GPR37 has been challenged and presently GPR37L1/GPR37 have regained their orphan status. Here we demonstrate that in their natural habitat, astrocytes, these receptors mediate a range of effects of TX14, including protection from oxidative stress. The Saposin C/GPR37L1/GPR37 pathway is also involved in the neuroprotective effect of astrocytes on neurons subjected to oxidative stress. The action of TX14 is at least partially mediated by Gi-proteins and the cAMP-PKA axis. On the other hand, when recombinant GPR37L1 or GPR37 are expressed in HEK293 cells, they are not functional and do not respond to TX14, which explains unsuccessful attempts to confirm the ligand-receptor pairing. Therefore this study identifies GPR37L1/GPR37 as the receptors for TX14, and, by extension of Saposin C, and paves the way for the development of neuroprotective therapeutics acting via these receptors.

Key words:

Neuroprotection, astroprotection, orphan receptors, GPR37L1, GPR37, Saposin C, prosaptide, astrocyte, PKA, cAMP

Introduction

Any new target for effective neuroprotective therapy must be actively explored as it may have major medical and societal impacts. Orphan G-protein coupled receptors (GPCRs) are particularly attractive because they are the most plausible targets for modern small molecule drugs, but this approach critically depends on identification of their endogenous agonists. The search for druggable targets in the brain conventionally focused on neurons, but astrocytes as natural neuroprotectors represent particularly attractive drug targets. Their neuroprotective mechanisms are numerous and include uptake of glutamate to prevent neurotoxicity, regulation of extracellular ions and pH, provision of anti-oxidative molecules (e.g. glutathione) and trophic factors, control micro-circulation, etc. (Liu *et al.*, 2017).

In 1994 peptide prosaposin (PSAP) and its fragment Saposin C (Sap C) were identified as neurotrophic factors using the neuroblastoma NS20 line and specific binding of radio-labelled Sap C with a Kd of 19 pM was demonstrated (O'Brien *et al.*, 1994). Soon it was shown that chronic icv infusion of recombinant PSAP almost completely prevented ischemia-induced learning deficits and neuronal loss in gerbils (Sano *et al.*, 1994) and the existence of a GPCR for the neuroprotective part of Sap C was thus postulated (Hiraiwa *et al.*, 1997). The experimental usefulness of SPAP and Sap C is limited by their length but luckily, the neuroactive part is rather short and can be mimicked by peptides known as prosaptides, of which the most studied is prosaptide TX14(A). The sequence of TX14(A) is highly evolutionarily conserved (Fig. S1). Although neuroprotective effects of PSAP fragments were demonstrated in several models *in vitro* and *in vivo* (Campana *et al.*, 1998;Hozumi *et al.*, 1999;Otero *et al.*, 1999;Gao *et al.*, 2016), the underlying mechanism remained unclear until 2013, when two closely related orphan receptors GPR37L1 and GPR37 (Leng *et al.*, 1999) were proposed to mediate the actions of PSAP and its mimetics (Meyer *et al.*, 2013).

GPR37L1 is highly expressed by astrocytes, which also express low levels of GPR37 (Fig S2, S3) (Zhang *et al.*, 2014;Marazziti *et al.*, 2007;Jolly *et al.*, 2017;Smith, 2015)). GPR37 is highly expressed in dopaminergic neurons and early work focused on the idea of GPR37 being involved in Parkinson's disease (Imai *et al.*, 2001;Cantuti-Castelvetri *et al.*, 2007;Marazziti *et al.*, 2007). The importance of GPR37L1 for brain function has been recently demonstrated in

humans. A point mutation in GPR37L1 leads to a severe neurological phenotype with includes intractable epilepsy, lethal in some of the affected individuals (Giddens *et al.*, 2017). GPR37L1- and especially double GPR37L1/GPR37-knockout mice were highly susceptible to seizures (Giddens *et al.*, 2017). Moreover, deletion of GPR37L1 drastically increased the neuronal loss after an ischemic stroke (Jolly *et al.*, 2017). These and other findings underscore the importance of GPR37L1 for brain health.

However, the pairing of GPR37L1/GPR37 with PSAP and TX14(A) (Meyer *et al.*, 2013) was later challenged. It was reported that these receptors are highly constitutively active and couple via Gs proteins, rather than the Gi pathway as originally reported (Meyer *et al.*, 2013). Moreover, on the background of their high constitutive activity, TX14(A) was ineffective (Coleman *et al.*, 2016;Giddens *et al.*, 2017;Ngo *et al.*, 2017). Regulation of this constitutive activity was suggested to occur via cleavage of the extracellular part of GPR37L1 (Mattila *et al.*, 2016;Coleman *et al.*, 2016). These reports reinforced the skepticism based on the failure of TX14(A) to activate GPR37L1/GPR37 using the DiscoverX orphan receptor screening panel (Smith, 2015;Southern *et al.*, 2013). Importantly, all studies reporting high constitutive activity of GPR37L1 and GPR37 and lack of TX14(A) agonism relied on expression of recombinant GPR37L1 in either HEK293 or CHO cells (Ngo *et al.*, 2017;Giddens *et al.*, 2017;Southern *et al.*, 2013) or yeast (Coleman *et al.*, 2016).

Thus, the nature of the endogenous agonist of GPR37L1 and GPR37 is currently elusive.

High constitutive activity of GPR37L1/GPR37 should lead to persistent production of copious amounts of cAMP. However, this has never been noticed in astrocytes where GPR37L1 is particularly abundant (Fig S2, S3). To the contrary, astrocytes vigorously respond to stimuli which increase cAMP production (such as agonists of Gs-coupled receptors or low concentrations of forskolin), indicating that their resting levels of cAMP are not anywhere near saturation, see for example (Goldman & Chiu, 1984;Tardy *et al.*, 1981;Clark & Perkins, 1971) and numerous other studies.

We hypothesized that coupling of GPR37L1/GPR37 in transiently transfected cell lines does not reveal their true physiological signaling and re-evaluated them in their natural habitat, the astrocytes. Our findings demonstrate that PSAP is, indeed, the natural ligand of

GPR37L1/GPR37 and pave the way for development of neuroprotective drugs based on this signaling system.

Materials and Methods

Primary cultures of astrocytes and cortical neurons

Experiments were performed in accordance with the UK Animals (Scientific Procedures) Act, 1986 and were approved by the University of Bristol ethics committee.

Astrocytes: Primary cultures of astrocytes were prepared from the cerebral cortices, cerebellum and brainstem from Wistar rat pups (P2) following protocols described previously (1-3). Briefly, the brains of Wistar P2 pups were dissected out, crudely cross-chopped and bathed in a solution containing HBSS, DNase I (0.04 mg/ml), trypsin from bovine pancreas (0.25 mg/ml) and BSA (3 mg/ml). The preparation was agitated at 37 °C for 15 mins. Trypsinization of the brain tissue was terminated by the addition of equal volumes of culture media comprised of DMEM, 10% heat-inactivated FBS, 100 U/ml penicillin and 0.1 mg/ml streptomycin and then centrifuged at 2000 rpm, at room temperature (RT) for 10 mins. The supernatant was aspirated, and the remaining pellet was resuspended in 15 ml HBSS containing BSA (3 mg/ml) and DNase I (0.04 mg/ml) and triturated gently. After the cell debris had settled, the cell suspension was filtered through a 40 µm cell strainer (BD Falcon) and cells were collected after centrifugation. Cells were seeded in a T75 flask containing culture media (see above) and maintained at 37 °C with 5% CO2. Once the cultures reached confluence and one week later, the flasks were mildly shaken overnight to remove microglia and oligodendrocytes. When astrocytes were seeded for experiments, media was changed to DMEM supplemented with 5% FBS instead of 10% FBS. This is to reduce the content of PSAP in the culture media hence make PSAP depletion easier to achieve. Please note there was no difference in cell growth in the media containing either 5% or 10% FBS.

Neurons: Cerebral cortices were dissected out from a litter (8-12) of Wistar rat embryos on gestation day 18 (E18) and collected in dissection saline (HBSS, 25.6 mM glucose, 10 mM

159 $MgCl_2$, 1 mM Hepes, 1 mM kynurenic acid, 0.005% phenol red, 100 U/ml penicillin, 0.1
160 mg/ml streptomycin). Meninges were removed, and tissues were chopped into pieces <1
161 mm3 and dissociated in 0.25% Trypsin in dissection saline in the presence of 3 mg/ml BSA at
162 37°C for 15 mins. An equal volume of plating media (Neurobasal A with 5% horse serum, 2%
163 B27, 400 nM L-glutamine, 100 U/ml penicillin, 0.1 mg/ml streptomycin) was added to
164 terminate the dissociation. Cells were pelleted at 2000 rpm for 5 mins at room temperature,
165 resuspended in plating media, and triturated gently. The cell suspension was diluted
166 appropriately and passed through a 40 µM cell strainer. $1x10^5$ cells per well were plated on
167 poly-D-lysine-coated glass cover slips in 24-well plates. Two hours later, the plating media
168 was replaced with feeding media (Neurobasal A with 2% B27, 800 nM L-glutamine, 20 U/ml
169 penicillin, 20 µg/ml streptomycin). On day 5, half of the media was replaced with feeding
170 media in which glutamine was replaced with 4 µM Glutamax. The antimitotic cytosine β-D-
171 arabinofuranoside (10 µM) was added to control glial contamination. Neurons were used for
172 experiments 10 days later.

173 Neuron/astrocyte co-cultures: Neurons were prepared (see above) and plated at 1x105 cells
174 per well on poly-D-lysine-coated glass coverslips in 24 well plates. Astrocyte inserts were
175 prepared by plating astrocytes on poly-D-lysine-coated cell culture inserts with 1 µm
176 diameter pores (Greiner Bio-One) in the same serum-free media as used for neurons.
177 Astrocyte inserts were introduced into neuronal cultures as required. The separation
178 between both cell types allowed secreted molecules to freely diffuse while preventing direct
179 astrocyte-to-neuron contact.

180

181 **Real Time PCR on primary cultured and acutely isolated astrocytes**

182 In order to verify that the expression of GPR37L1 and GPR37 in our cultured astrocytes is
183 not an result of *in vitro* conditions, we performed acute vibro-isolation of cortical astrocytes
184 frim P12 rats using a method recently described by Lalo and Pankratov(Lalo & Pankratov,
185 2017). ~50 single astrocytes were manually collected from the bottom of a small Petri dish
186 into a sterile test tube. Power SYBR Green Cells-to-Ct Kit (Ambion) was used to reverse
187 transcription directly from cultured cell lysates, without isolating RNA. The resulting cDNA
188 samples were then analysed using QuantiTect SYBR green PCR kit (Qiagen) on DNA Engine

OPTICON 2 continuous fluorescence detector, following the manufacturer's protocol. β-actin was used as a reference house-keeping gene. All primers were designed to span at least one intron and to produce products of ~100 bp and pre-validated for their efficiency. Products of PCR reaction were resolved on agarose gel to confirm their sizes (Fig. S3). Sequences of the primers are shown below.

β-Actin forward: CTAAGGCCAACCGTGAAAAG

reverse: GGCATACAGGGACAACACAG

GPR37L1 forward: ATGTTTCTTGCCGAGCAGTG

GPRF37L1 reverse: CCACATGGAATCGGTCTATG

GPR37 forward: TCCATGAGTTGACCAAGAAG

GPR37 reverse: CTATGCACAGTGCACATAAG

GFAP forward: GAGAGGAAGGTTGAGTCGCT

GFAP reverse: CACGTGGACCTGCTGCTG

Western blotting

For verification of GPR37L1/37 knock down viral vectors AVV-CMV-EmGFP-miR155/GPR37L1 and AVV-CMV-EmGFP-miR155/GPR37, transduced astrocytes were harvested and placed on ice and washed with ice-cold phosphate-buffered saline (PBS). The membrane proteins were then extracted using the Mem-PER eukaryotic membrane protein extraction reagent kit (PIERCE) and purified with SDS-PAGE sample preparation kit (PIERCE). After quantification with BCA protein assay kit (PIERCE), 20 μg of membrane protein per lane were fractionated on a 4–12% Bis-Tris gel (NuPage 4–12% Bis-Tris Gel, Life Technologies), and transferred to a polyvinylidene difluoride (PVDF) membrane (Millipore). After blocking with 5% non-fat dry milk (NFDM) in Tris-buffered saline with 0.1% tween-20 (TBST) buffer for 45 mins at RT, the PVDF membrane was cut into two parts at 100KD-size level. The part of the membrane containing small sized proteins was incubated with primary antibody to GPR37L1 (1:1000 dilution) or GPR37 (1:1000 dilution) in 3% NFDM-TBST at 4℃ overnight, and the other part of membrane was incubated with primary antibody to pan-cadherin (120Kda) (1:2000

dilution) as a membrane protein loading control, in 3% NFDM-TBST at 4°C overnight. Following incubation with horseradish peroxidase conjugated secondary antibody (DAKO, 1:2000 dilution) for 90mins at RT, the immunoreactivities were detected with Immun-Star Western C chemiluminescent kit (Bio-Rad). For the PSAP depletion assay and the proof of the existence of PSAP in serum-supplemented culture media, we used the same protocol as described above except that 5 µl of media or elution from protein A magnetic beads was applied as the sample volume. A polyclonal rabbit anti-PSAP antibody was employed. For Western blotting of PSAP in neuron-astrocyte co-culture media, we changed to the Amersham ECL Plex western blotting system using a low-fluorescent PVDF membrane (GE Healthcare) and Alexa Fluor 488 secondary antibody-conjugated goat anti-rabbit. Protein transfer and membrane blocking was the same as in the above protocol. Membranes were incubated with anti-PSAP (1:500 dilution) overnight at 4 °C. Secondary antibody Alexa Fluor 488 was incubated for one hour in the dark at room temperature. Before imaging, the membrane was thoroughly washed. Signal was detected by scanning the membrane on a fluorescent laser scanner (Typhoon, GE Healthcare).

Generation of knock-down adenoviral vectors (AVV)

AVV for the knock-down experiments were based on a modified Pol II miR RNAi Expression Vector system (Invitrogen) and our previous work (Liu *et al.*, 2010). Three AVV were constructed, namely, AVV-CMV-EmGFP-miR155/GPR37L1, AVV-CMV-EmGFP-miR155/GPR37 and AVV-CMV-EmGFP-miR155/negative. The first two were used for knocking down GPR37L1 and GPR37 in astrocytes, respectively. The third one is a negative control, harboring a miRNA sequence that can form a hairpin structure that is processed into mature miRNA but is predicted not to target any known vertebrate gene. All three vectors were made based on BLOCK-iT™ Pol II miR RNAi Expression Vector Kit with EmGFP (Invitrogen). This system supports chaining of miRNAs, thus ensuring co-cistronic expression of multiple miRNAs for knock down of a single target. Three sets of two complementary single-stranded DNA microRNA sequences (targeting different regions of the same gene) for GPR37L1 and GPR37 were designed by the BLOCK-iT™ RNAi Designer (Invitrogen). The complementary single-stranded oligos were then annealed and cloned into the linearized pcDNA™6.2-GW/EmGFP-miR vector. The pre-miRNA expression cassettes were transferred into an

adeno shuttle plasmid pXcX-Sw-linker (Duale *et al.*, 2005), resulting in construction of pXcX-CMV-EmGFP-miR155/GPR37L1, pXcX-CMV-EmGFP-miR155/GPR37 and pXcX-CMV-EmGFP-miR155/negative. AVV were then produced by homologous recombination of shuttle and the helper plasmid pBHG10 in HEK293 cells. The media was collected for subsequent rounds of AVV proliferation in HEK293 cells until cytopathic effects were achieved. AVV were purified using CsCl gradient protocols. Titers were established using an immunoreactivity spot assay as described previously (Duale *et al.*, 2005).

PSAP depletion

To deplete PSAP from culture media (DMEM supplemented with 5% FBS), initially, 25 µl of Protein A Magnetic Beads (NEB) per 200 µl media were added and incubated for 1 hour at 4°C. Magnetic field was applied for 30 seconds to pull beads to the side of the tube and the supernatant was transferred to a new tube. This step is required to remove non-specific binding proteins. Then, 5 µl of anti-PSAP antibody (500 µg/ml) were added to the supernatant and incubated for 1 hour at 4°C. Protein A Magnetic Beads were used again to pull down the antibody-bound PSAP. Western blot was used to verify the efficient removal of PSAP which could then be recovered from the beads (Fig. S4).

cAMP assays

Two types of detection were used.

Luminescence activity-based GloSensor assay (Promega). The GloSensor assay uses genetically encoded biosensor variants with cAMP binding domains fused to mutant forms of Photinus pyralis luciferase. The luminescence of the reporter increases directly proportionally to the amount of cAMP present. Astrocytes were seeded in 96-well plates and transduced with an AVV bearing the CMV-driven GLO22F. at multiplicity of infection (MOI) 10. Advice and assistance of Dr HJ Bailes HJis acknowledged. 24 hours after transduction, media was exchanged for 100 ul HEPES-buffered HBSS (pH7.6). Cells were then incubated with 0.731mMbeetle luciferin for 2 hours in the dark. After baseline reading, NKH477 and/or TX14(A) were added to the wells and incubated for 20 mins. Luminescence measurements were obtained using a Tecan microplate reader (Infinite M200 PRO).

FRET-based cAMP assay: Two to three days prior to recordings, astrocytes were plated onto coverslips in prosaposin-depleted media (PDM) and transduced with an AVV to express an Epac [Exchange protein directly activated by cAMP)-based FRET sensor (kindly provided by Jalink K, Amsterdam(Klarenbeek *et al.*, 2015;Klarenbeek & Jalink, 2014)] specifically in astrocytes. PDM was exchanged daily. For recording, coverslips were placed into a chamber on a confocal microscope and continuously superfused with HEPES-buffered solution (HBS; in mM: NaCl 137, KCl 5.4, Na_2HPO_4 0.34, KH_2PO_4 0.44, $CaCl_2$ 1.67, $MgSO_4$ 0.8, $NaHCO_3$ 4.2, HEPES 10, Glucose 5.5; pH 7.4, 31.4°C). After taking baseline readings of astrocytes in the field of view, cells were exposed to 5 mins of NKH477 (0.5 µM), alone or in combination with TX14(A) (100 nM). Fluctuations in cAMP were monitored through CFP/YFP (465-500nm/515-595nm bands) emission ratios upon 458 nm light excitation. Images were acquired every 4 seconds. All FRET ratios were normalized to baseline.

PRESTO-Tango β-arrestin-recruitment assay

To measure receptor activation, the PRESTO-Tango β-arrestin-recruitment assay was performed as previously described, with modifications (Kroeze *et al.*, 2015). HTLA cells, a HEK293 cell line stably expressing a tTA-dependent luciferase reporter and a β-arrestin2-TEV fusion gene, were used. The cells were maintained in DMEM media supplemented with 10% FBS, 100 U/ml penicillin and 100 µg/ml streptomycin, 2 µg/ml puromycin and 100 µg/ml hygromycin B. For transfection, HTLA cells were plated in 96-well white polystyrene plates (Greiner Bio-One) in DMEM media supplemented with 10% FBS, 100 U/ml penicillin and 100 µg/ml streptomycin at a density of $4x10^5$ cells/ml. For measuring activation of GPR37 and GPR37L1 by TX14(A) stimulation, PDM was used instead. After 16 hours, cells were transfected with the plasmid containing the GPR37 or GPR37L1 ORF (Addgene) using Trans-IT 293 (Mirus) according to manufacturer's protocol. On the next day, drugs were added in assay buffer (20 mM HEPES in HBSS, pH 7.4) and left to incubate for 24 hours. Solutions were aspirated, and 80 µl per well of Bright-Glo solution (Promega) diluted 20-fold in assay buffer was added to each well in the dark. Following 20 mins of incubation, luminescence measurements were obtained using a Tecan microplate reader (Infinite M200 PRO).

Scratch Wound Assay

A wound recovery assay was carried out to analyze the migration of astrocytes using the IncuCyte system (Essen BioScience). Primary astrocytes were seeded in ImageLock 96-well plates (4379, Essen BioScience) at a density of $4x10^4$ per well. After 24 hours, standardized and reproducible (700-800 μm wide) scratch 'wounds' were created in all wells using a dedicated device. Cultures were exposed to different testing conditions, e.g. stressors, and were maintained and imaged at hourly intervals up to 72 hours.

Cell density was measured in the scratch area and compared to undisrupted adjacent monolayer. Relative wound density (%), a measure of wound recovery, was calculated using the formula: Relative wound density (%) = (density of wound region at certain time point – initial density of wound region)/(density of intact cell region at certain time point - initial density of wound) x 100.

DAPI staining

Astrocytes were seeded in 96-well plate ($1x10^4$ per well) and fixed in 4% paraformaldehyde for 5 mins, washed in PBS three times for 5 mins each time before and after incubating with 1 μg/ ml DAPI for 10 mins. Round and whole nuclei in 9 fields of view per well were counted using ImageJ.

BrdU Incorporation Assay

In order to detect cell division, astrocytes were seeded in a 96-well plate ($4x10^3$ per well) in media supplemented with 5% FBS or PDM and cultured for one day. BrdU was added to the wells at a final concentration of 10 μM. 24 hrs later, cells were fixed with 4% paraformaldehyde in PBS (pH 7.4) for 10 mins at room temperature and permeabilized with 0.1~0.25% Triton X-100 in PBS. Cells were then incubated with 1 M HCl for 30 mins, followed by primary antibody incubation with mouse monoclonal anti-BrdU antibody (1:100) containing 2.5% goat serum at 4℃ overnight. Before imaging, cells were incubated with Alexa Fluor 488-conjugated goat anti-mouse secondary antibody for 30 mins at room temperature.

Lactate dehydrogenase (LDH) release assay

LDH release from damaged cells was assessed calorimetrically with LDH Cytotoxicity Assay Kit (Pierce) according to the manufacturer's instructions. Activity is proportional to colorimetric reduction of tetrazolium salt measured at 490 nm. Cytotoxicity was normalized to maximal LDH activity as released from cells acutely exposed to Triton X-100, and calculated using the formula: % Cytotoxicity = (Compound-treated LDH activity – Spontaneous LDH activity)/(Maximum LDH activity – Spontaneous LDH activity) × 100.

To determine the protective effect of prosaptide TX14(A) against oxidative stress on primary astrocytes, cells were seeded in triplicates in 96-well plates ($4x10^4$ per well) in PDM and transduced with AVV-CMV-EmGFP-miR155/negative (labelled as miRNA-negative in the figures), or a mixture of AVV-CMV-EmGFP-miR155/GPR37L1 and AVV-CMV-EmGFP-miR155/GPR37 (molar ratio 3:1, labeled as miRNA-GPR37L1/GPR37 in figures). 24 hours later, the media was replaced by fresh PDM and cells were treated with H_2O_2 (250 μM), staurosporine (200 nM) and rotenone (100 μM) for 5 hrs in the presence or absence of TX14(A). The media was then replaced by fresh PDM with or without TX14(A). Cells were incubated for a further 24 hours before carrying out the LDH reaction on 50 μl of media.

For the protective effect of astrocytes on stressed neurons in the co-culture system, astrocytes or neurons were transduced with AVV at MOI 10. For astrocytes, cells were transduced at the time of plating on cell culture inserts. For neurons, cells were transduced on day 3 after preparation and then plated. 24 hrs later, media were replaced. Cells were cultured for 7 more days before they were treated with H_2O_2 (250 μM, 1 hr), rotenone (50 μM, 2 hrs) or staurosporine (100 nM, 2 hrs). Stressors were then removed and neurons were incubated with or without astrocytes inserts. 24 hrs later, the LDH reaction was using 50 μl of media. Cytoprotection was calculated using the formula: % Cytoprotection = % cytotoxicity in the control condition - %cytotoxicity in the experimental conditon.

Reagents

Cell culture and cell-based assays related: Beetle luciferin potassium salt (E1602, Promega); B27 (17504044, Life Technologies); Bovine serum albumin (BSA) fraction V (A3294, Sigma); BrdU (AB142567, Abcam); Bright-Glo™ reagent (E2610, Promega); Cytosine β-D-arabinofuranoside (C1768, Sigma); DNase I (D5025, Sigma); DAPI (D9542, Sigma); Dulbecco's Modified Eagle Medium (DMEM) (61965, Life Technologies); Fetal Bovine Serum (FBS, 10082147, Life Technologies); GlutaMax (35050038, Life Technologies); L-Glutamine (2503008, Life Technologies); Hank's Balanced Salt Solution (HBSS) (14175-129, Invitrogen); HEPES (H3375, Sigma); Horse serum (H1138, Sigma); Hygromycin B (H3274, Sigma); Kynurenic acid (K3375, Sigma); Neurobasal-A media (10888022, Life Technologies); Penicillin/Streptomycin (15140-122, Life Technologies); Poly-D-Lysine (A-003-E, Millipore); Protein A Magnetic Beads (NEB, S1425S); Puromycin (P8833, Sigma);Triton X-100 (T8787, Sigma); Trypsin (type III, bovine fraction) (T9935, Sigma). Ambion Power SYBR Green Cells to Ct kit (4402953) was used to verify GPR37L1 and GPR37 expression in cultured and acutely isolated astrocytes.

Antibodies: Alexa Fluor 488-conjugated goat anti-rabbit secondary antibody (R37116, Life Technologies); Alexa Fluor 488-conjugated goat anti-mouse secondary antibody (R37120, Life technologies); GPR37 L1 antibody (AB151518, Abcam); GPR37 antibody (14820-1-AP, Proteintech); mouse monoclonal anti-BrdU antibody (GTX27781, GeneTex); pan-cadherin antibody (AB6529, Abcam); rabbit anti-PSAP antibody (AB68466, Abcam).

Drugs: 6-BenZ-cAMP (B009-10, BIOLOG Life Science Institute); 8-pCPT-2'-O-Me-cAMP (C041-05, BIOLOG Life Science Institute); H_2O_2 (H1009, Sigma); Pertussis toxin (3097, Tocris); NKH 477 (SC-204130, Santa Cruz Biotechnology); Prosaptide TX14(A) (5151, Tocris); Rotenone (R8875, Sigma); Staurosporine (10042804, Fisher).

All other chemicals were from Sigma.

Statistical Analysis

All data analysis was performed with GraphPad Prism 7 (GraphPad Software Inc.). One-way ANOVA with one of the post-hoc analysis was used, unless otherwise stated. *$p<0.05$,

392 **p<0.01, ***p<0.001, ****p<0.0001. Grouped data are presented as mean ± SD, unless
393 otherwise stated.

394 Further details of statistical procedures can be found in the associated Excel file
395 “Supplemental Statistics”.

396

397

RESULTS

GPR37L1/GPR37 activation by prosaptide inhibits cAMP production in astrocytes but not in HEK293 cells

Consistent with published information, GPR37L1 is strongly expressed by cultured rat astrocytes which also express GPR37 at a lower level. We have also confirmed that both receptors are present in acutely isolated cortical astrocytes from P12 rats, consistent with various published transcriptomes (Fig S2,3). Therefore, we always targeted both receptors simultaneously. A powerful double knock-down of GPR37L1 and GPR37 was achieved by modifying conventional micro-RNA based cassettes to incorporate 3 anti-target hairpins fused to the 3'-end of the Emerald green protein (Fig. 1A; (Liu *et al.*, 2010)). These "triple-hit" cassettes suppressed GPR37L1 and GPR37 protein expression below our detection limits while a negative control sequence had no impact (Fig 1B). The efficacy of the knock-down was additionally confirmed using Real Time PCR (Fig S5). To ensure maximal transduction of astrocytes we used adenoviral vectors (AVV) which are exceptionally effective tools for these cells (Fig S6).

To assess intracellular cAMP changes, AVV were also used to express the Glosensor biosensor (Promega™). Baseline levels of cAMP were raised ~20-fold using a water soluble forskolin analogue, NKH477. On that background, TX14(A) concentration-dependently decreased cAMP with an IC_{50} of 17.8 nM (Fig. 1C). The maximal concentration of TX14(A) used (200 nM) inhibited NKH477-mediated cAMP production by approximately 40% (Fig. 1C). The decrease of cAMP induced by TX14(A) was pertussis toxin (PTX) sensitive (Fig. 1D). Expression of the negative control miRNA vector had no effect while combined knock-down of the GPR37L1 and GPR37 receptors completely obliterated the TX14(A)-mediated decrease in cAMP levels (Fig. 1C). In addition, we employed an EPAC-based high affinity FRET sensor for cAMP (Klarenbeek *et al.*, 2015) to visualize cAMP dynamics following TX14(A) application and found that TX14(A) (100 nM) significantly reduced the NKH477-evoked rise in FRET ratio (Fig. 1 E,F).

Several previous reports which failed to confirm the TX14(A) effect on GPR37L1 and GPR37 used transiently transfected HEK293 cells. To verify that in HEK293 cells GPR37L1 and GPR37

signaling is different to that in astrocytes (Fig. 1 C-F), we used the PRESTO-Tango system (Kroeze *et al.*, 2015). It provides GPCRs adapted for transient expression in a HEK293 line, modified to detect agonist-induced GPCR internalization. In that assay, GPR37 was constitutively active (compared to the baseline with ADRA1, Fig. S7) and both receptors were insensitive to prosaptide TX14(A) (Fig. 2), while the α-adrenoceptor 1a (ADRA1a) demonstrated an appropriate response (Fig. S7). The most likely explanation for this difference is that GPR37L1 and GPR37 require some additional proteins for their correct function which are lacking in HEK293 cells. Further analysis of this issue is outside of the scope of the current study.

PSAP and TX14(A) acting via GPR37L1/GPR37 are essential for the motility of astrocytes

Body fluids such as milk, blood and cerebrospinal fluid, contain PSAP (Kishimoto *et al.*, 1992). Most media used for culturing are supplemented with fetal bovine serum (FBS). Unsurprisingly, PSAP was present in FBS-supplemented media (Fig. S4). We studied the effect of PSAP depletion, using immunoadsorption (Fig. S4), on the motility of astrocytes in a wound scratch assay. Reproducible (700-800 µM wide) scratch wounds were created in astrocyte monolayers. In FBS-containing media, the wound essentially closed within 48 hours (Fig. 3A; Suppl movie 1). This process was drastically slowed down by PSAP depletion. 100 nM TX14(A) almost completely compensated for the loss of PSAP (Fig. 3A-C; Suppl movies 2 and 3). Importantly, knock-down of GPR37L1/GPR37 in astrocytes blocked the ability of TX14(A) to facilitate wound closure while the control vector was ineffective (Fig. 3C, Suppl movies 4 and 5). Astrocytes divide in culture, albeit very slowly, but neither depletion of PSAP nor addition of TX14(A) affected the number of cells in cultures (Fig. 3D) nor the number of newly divided cells based on BrdU staining (Fig. 3E). Therefore, the effects of PSAP and TX14(A) in the scratch assay are due to their effect on the motility of astrocytes.

Stimulation of adenylate cyclase with NKH477 (1 to 10 µM) greatly slowed down wound closure, as did the cAMP analogue 6-benz-cAMP (250 to 1000 µM), a selective PKA activator, in a concentration-dependent manner (Fig. 4A). The cAMP analogue 8-pCPT-2'-O-Me-cAMP (250 to 1000 µM) which specifically activates EPAC (cAMP-GEF) had no effect (Fig. 4A). Interestingly, non-selective stimulation of cAMP production by NKH477 as well as

457 stimulation of PKA by 6-BenZ-cAMP and of EPAC by 8-pCPT-2'-O-Me-cAMP reduced
458 proliferative activity of astrocytes (Figs. 3D, 4B). Since all three cAMP raising drugs had a
459 similar effect on cell numbers but different effects on wound closure dynamics, there
460 appears to be no direct relationship between these two effects of cAMP. Taken together,
461 the data indicate that the key mechanism of wound closure which is regulated via the
462 GPR37L1/GPR37 axis is the lateral movement of astrocytes, rather than their division.

463 **PSAP and prosaptide protect astrocytes from oxidative stress damage via GPR37L1/GPR37**

464 Exposure of astrocytes to H_2O_2, rotenone or staurosporine drastically inhibited their ability
465 to close the wound in PSAP-depleted media but TX14(A) rescued the stressed astrocytes'
466 wound closure capacity (Fig. 5A). This effect of TX14(A) was eliminated by the knock-down
467 of GPR37L1/GPR37 in astrocytes, while the control knock-down vector was ineffective (Fig.
468 5A).

469 It has been previously reported that the death of cortical astrocytes triggered by H_2O_2 can
470 be reduced by TX14(A) (Meyer *et al.*, 2013). We adjusted concentrations and exposure time
471 of H_2O_2, rotenone and staurosporine to evoke a comparable degree of cytotoxicity as
472 assessed by LDH release assay (Fig. 5B). In PSAP-depleted media, neither GPR37L1/GPR37
473 knock-down, nor the negative control vector, changed the cytotoxic impact of stressors.
474 TX14(A) strongly reduced cytotoxicity which was particularly prominent in the case of
475 staurosporine, and this was prevented by GPR37L1/GPR37 knock-down (Fig. 5B).

476 **Astrocytic GPR37L1/GPR37 signaling contributes to the protection of the cortical neurons**
477 **from damage by oxidative stressors**

478 Neuronal cultures were subjected to the same oxidative stressors as above and conditions
479 were adjusted to trigger a comparable degree of damage, based on LDH release. After
480 removal of the stressors, astrocytes were introduced into the wells on elevated membranes,
481 thereby preventing direct cell-cell contact (Fig. 6A). Astrocytes exerted a strong protective
482 effect on the neurons which was directly proportional to the quantity of astrocytes (Fig. 6B;
483 Fig. S8). 75k astrocytes per well provided a near-maximum neuroprotective effect and this
484 astrocyte density was used for further experiments.

TX14(A) applied directly to damaged cultured neurons at 100 nM, provided a slight but significant protection against the stressors (Fig. 6C). This indicates that either neuronal GPR37L1/GPR37 receptors, or the few astrocytes remaining in the neuronal cultures, could be contributing to the neuroprotective actions of PSAP.

Fig. 6D demonstrates that, for each of the 3 stressors, co-culturing with astrocytes reduced LDH release by ~35 - 45%. Importantly, the media used in these experiments was FBS-free and contained no added PSAP. However, when anti-PSAP antibodies were added, the cytoprotective effect of astrocytes was dramatically reduced (Fig. 6D). This strongly suggests that endogenous PSAP (or Sap C) in the co-culture system is important for the cytoprotective effect of astrocytes. We were able to immunodetect directly the increase in PSAP in co-culture media in response to H_2O_2 stress applied to neurons (Fig. S9), although the cellular source of this the stress-induced PSAP surge is currently unknown. Knock-down of GPR37L1/GPR37 selectively in astrocytes limited astrocyte-mediated neuroprotection to a degree comparable to PSAP depletion (Fig. 6D). Interestingly, application of the same knock-down AVV to neurons had no effect. These results are consistent with the idea that stress-induced PSAP release and astrocytic GPR37L1/GPR37 signaling are critical for PSAP action.

Discussion

The key message of this study is that the original coupling of PSAP and its prosaptide fragments to GPR37L1 and GPR37 suggested by (Meyer *et al.*, 2013) was correct. This implies that we can expect small molecules based around the structure of TX14(A) be astro- and neuroprotective.

Neuroprotection by PSAP

The first cells, used to demonstrate a protective potential of PSAP were mouse neuroblastoma NS20Y and human neuroblastoma SK-N-MC cells (O'Brien *et al.*, 1994). Interestingly, the neuroblastoma lines closely related to SK-N-MC express substantial levels of GPR37 (Harenza *et al.*, 2017). Published transcriptomes of astrocytes (Zhang *et al.*, 2016;Zhang *et al.*, 2014;Anderson *et al.*, 2016;Chai *et al.*, 2017) and our own data (Fig S2,3) unequivocally demonstrate that astrocytes of various parts of the central nervous system express high levels of GPR37L1 while the level of GPR37 is generally much lower. Cytoprotective and "trophic" effects of PSAP and its fragments were found in diverse models and species. Prosaptides improved the outcome of sciatic nerve damage in guinea pigs (Kotani *et al.*, 1996a), alleviated the ischemia-induced memory deficits in gerbils (Kotani *et al.*, 1996b), reduced neuropathy in diabetic rats (Calcutt *et al.*, 1999), and the behavioral and anatomical detriments caused by brain wound insult in rats (Hozumi *et al.*, 1999). A stabilized TX14(A)-like peptide, retro-inverso prosaptide D5, was neuroprotective in rats (Lu *et al.*, 2000) and ameliorated hyperalgesia in a model of neuropathic pain (Yan *et al.*, 2000). The neuroprotective effects of TX14(A) were confirmed by another group (Jolivalt *et al.*, 2006;Sun *et al.*, 2002;Jolivalt *et al.*, 2008). An 18-amino acid long prosaptide was also protective in a model of dopaminergic neuron damage (Sun *et al.*, 2002;Gao *et al.*, 2013). Therefore, there is solid evidence for the neuroprotective potential of this pathway.

PSAP-GPR37L1/GPR37 pairing

All these effects obviously called for the development of a neuroprotective therapy, but this opportunity could not be realized in the absence of cognate receptors. The study by (Meyer *et al.*, 2013) strongly suggested that these are the orphan receptors GPR37L1 and GPR37. Some of the effects were demonstrated in HEK293 cells, but the most striking protective effect of TX14(A) was observed in cultured astrocytes. The findings of (Meyer *et al.*, 2013)

were later criticized, the key concerns being the high concentration of TX14(A) used, the small magnitude of the G_i-mediated inhibitory effect on cAMP concentration and the failure to detect TX14(A) agonism in a β-arrestin-based DiscoverX assay (Southern *et al.*, 2013;Smith, 2015). Other recent studies reported high constitutive activity of GPR37L1 and GPR37 and lack of a TX14(A) effect in either HEK293 cells or yeast (Ngo *et al.*, 2017;Giddens *et al.*, 2017;Southern *et al.*, 2013;Coleman *et al.*, 2016).

Our findings, however, are consistent with the conclusions drawn by (Meyer *et al.*, 2013). The presence of PSAP in the media or addition of TX14(A) had a powerful effect on astrocytic motility and protected them against oxidative stressors. In all cases this action could be completely prevented by knocking down GPR37L1/GPR37 (Figs. 3A-C, 5). Moreover, when astrocytes were used to rescue neurons subjected to oxidative stress, removal of GPR37L1/GPR37 only from astrocytes was sufficient to significantly weaken their neuroprotective capacity and block the protective action of TX14(A) (Fig. 6D). TX14(A) at a fairly high concentration (100 nM) had a weak direct protective effect on stressed neurons which is unlikely to make a major contribution to the neuroprotection seen in the presence of astrocytes (Fig. 6C). At least, application of the knock-down strategy to neurons was without an obvious effect (Fig. 6D).

Therefore, by several approaches, we demonstrate that the effects of PSAP and TX14(A) on astrocytes are invariably dependent on GPR37L1/GPR37. The partial protection provided to injured neurons by co-cultured astrocytes to some extent also depends on this signaling pathway. Given that only removal of GPR37L1/GPR37 from astrocytes, but not neurons interfered with neuroprotection in this paradigm, the likeliest scenario is that PSAP acts as an autocrine signal on the receptors located on the astrocytes to recruit additional, unidentified, neuroprotective molecules (Fig. 7).

Previous studies in mice lacking either of the two receptors demonstrated various, albeit relatively mild, phenotypes but, to the best of our knowledge, the possibility of compensation by the remaining receptor in a single knockout scenario has never been explored. This could be the reason why the pro-seizure phenotype of double GPR37L1/GPR37 knockout mice is so severe (Giddens *et al.*, 2017). Recent demonstration of a lethal neurological phenotype in humans with a point mutation in GPR37L1 (Giddens *et al.*, 2017) suggests that GPR37L1 is potentially indispensable for the health of the human

brain. A drastic increase in neuronal loss after an ischemic stroke in GPR37L1 knockout mice (Jolly *et al.*, 2017) further reinforces the importance of these receptors.

Coupling

The first study to indicate that a G_i-coupled receptor may mediate the action of PSAP found that pretreatment with PTX inhibited agonist-stimulated binding of [^{35}S]-GTPγS (Hiraiwa *et al.*, 1997). Strikingly, it also demonstrated that Sap C interacts with a receptor of ~54 kDa, corresponding almost exactly to the molecular mass of GPR37L1(Giddens *et al.*, 2017). In our study in astrocytes, TX14(A) inhibited cAMP production by approximately 40% from an elevated level set by the forskolin analogue (Glosensor assay). The effect of TX14(A) was PTX sensitive and the IC_{50} compares with that of numerous other GPCR agonists. Removal of GPR37L1 and GPR37 completely prevented the effect of TX14(A). These results confirm the original report (Meyer *et al.*, 2013) that GPR37L1/GPR37 are G_i-coupled receptors. Coupling to other G-proteins needs to be investigated further.

In the wound scratch assay, PSAP and TX14(A) were permissive to the spread of astrocytes into the barren area. This was due to an effect on lateral motility (Fig. 3D-E). Again, this effect was completely prevented by knock-down of the two receptors (Fig. 3C). Interestingly, stimulants of the cAMP pathway, the adenylyl cyclase activator NKH477, and two pathway-biased agonists, 6-BenZ-cAMP and 8-pCPT-2'-O-Me-cAMP, reduced the speed of division of cultured astrocytes (Fig 4B) but only 6-BenZ-cAMP which predominantly activates PKA (Bos, 2003) concentration-dependently suppressed spread of the astrocytes into the wounded area (Fig. 4A). Therefore, the motility of astrocytes is regulated by PKA, rather than EPAC-regulated proteins. TX14(A) did not interfere with the reduction in mitotic activity by either of the cAMP analogues (Fig. 4B). The mechanism by which PKA regulates astrocyte motility is currently unknown.

Controversy related to PSAP-GPR37L1/GPR37 pairing

Neither HEK293 cells nor yeast used in the recent conflicting studies (Ngo *et al.*, 2017;Giddens *et al.*, 2017;Coleman *et al.*, 2016) express GPR37L1 or GPR37 natively, nor were they ever demonstrated to be responsive to PSAP or prosaptides. These cells might not necessarily recapitulate the intracellular environment of astrocytes and neurons which

593 are the natural habitats of GPR37L1 and GPR37. Our experiments using PRESTO-Tango
594 confirmed that neither GPR37L1 nor GPR37 respond to TX14A in HEK293 cells (Fig. 2).

595 Serum-containing media can mask the effects of GPR37L1/GPR37 ligands because it
596 contains considerable levels of PSAP. Most likely astrocytes, neurons or both can secrete
597 some PSAP *in vivo*. This was visible in the "rescue" experiments where astrocytes reduced
598 the damage caused to neurons by added stressors. In these experiments anti-PSAP
599 antibodies reduced neuroprotection even though the media was nominally devoid of PSAP.
600 In the presence of stressed neurons, PSAP was greatly upregulated and easily detected in
601 the media by immunoblotting. Therefore, to fully reveal the agonist activity of TX14(A) it is
602 important to ensure that the receptors are not persistently exposed to endogenous or
603 media-derived PSAP.

604 Taken together, our results demonstrate that prosaptide TX14(A) (and, by extension, PSAP)
605 are the natural ligands of GPR37L1/GPR37 and confirm that in their native environment, the
606 astrocyte, these receptors couple to the G_i cascade as originally reported (Meyer *et al.*,
607 2013). Their native signaling is however, lacking or suppressed in cell lines (such as
608 transiently transfected HEK293 cells) used in β-arresting-based screening assays indicating
609 that for correct coupling GPR37L1 and GPR37 may require as yet unknown intracellular
610 partners present in astrocytes. This would not be a unique situation since some other
611 receptors, such as CGRP receptor, are known to require co-expression of receptor-
612 associated proteins. Of note, astrocytes express very high levels of syntenin-1, which is
613 important for trafficking of GPR37 (Dunham *et al.*, 2009). It is conceivable that its role
614 includes more than just trafficking. Given the powerful glio-protection and neuro-protection
615 mediated by these receptors and since GPCRs are the most "druggable" class of proteins
616 currently known, GPR37L1 (and GPR37, if they can be separated pharmacologically) become
617 highly valuable targets for development of novel neuroprotective therapies.

618

Figure legends

Fig. 1. TX14 (A) acting on GPR37L1/GPR37 reduces cAMP levels in astrocytes.

A: Layout of the adenoviral vectors for knock-down of GPR37L1 and GPR37. Each vector allows co-cistronic expression of three pre-miRNAs targeting different regions of the target gene. AVV: human adenoviral vectors serotype 5; CMV: human cytomegalovirus promoter; EmGFP: Emerald Green Fluorescent Protein; miR155: flanking pre-miRNA sequence derived from miR-155.

B: Western blot confirms that AVV-CMV-EmGFP-miR155/GPR37L1 and AVV-CMV-EmGFP-miR155/GPR37 (MOI 10) efficiently knock-down GPR37L1 and GPR37 in astrocytes. AVV-CMV-EmGFP-miR155/negative is a control vector with hairpin sequence relevant to no known vertebrate gene.

C: Concentration-response curves for inhibition of cAMP production by TX14(A) in astrocytes pre-treated with 1 µM NKH477. Cells were transduced with AVV-CMV-Glosensor and either AVV-CMV-EGFP (control), a mixture of AVV-CMV-EmGFP-miR155/GPR37L1 and AVV-CMV-EmGFP-miR155/GPR37 to knock-down GPR37L1/GPR37, or with AVV-CMV-EmGFP-miR155/negative (n= 4, triplicates).

D: AVV-CMV-Glosensor transduced astrocytes were pretreated with PTX (20 hrs, 100 ng/mL). 100 nM TX14(A)-induced cAMP reduction in astrocytes was PTX sensitive (n = 12, *** P <0.001 vs. indicated group, one-way ANOVA with Turkey's post-hoc analysis).

E: Astrocytes expressing an EPAC-based cAMP sensor were kept in PSAP-depleted media overnight and were stimulated with NKH477 (0.5 µM) in absence or presence of TX14(A) (100 nM). TX14(A) decreased the transient cAMP signal; average of 58 astrocytes from 4 experiments.

F: Pooled data from E shows significantly decreased FRET ratio peaks with TX14(A) (n=58= **** P < 0.0001, paired t-test).

Fig. 2.

GPR37L1 and GPR37 are non-responsive to prosaptide TX14-(A) in PRESTO-Tango assay in HEK293 cells.

PRESTO-Tango uses clones of numerous human GPCR, C-terminally tagged with a special signaling element. These receptors need to be expressed in a specially designed clone of

649 HEK293 cells. Agonist binding triggers receptor internalization and eventually leads to
650 expression of luciferase and luminescence. Two concentrations of plasmid DNA were used
651 to express the tagged receptors. GPR37 exhibits strong constitutive activity, especially when
652 using 0.1 µg/µl. Values obtained with 0.1 µg of GPR37 DNA could not be fitted with the
653 regression algorithm of Prizm software, hence no line is shown (n=6).

654 **Fig. 3. PSAP/GPR37L1/GPR37–mediated signaling is essential for migration of astrocytes in**
655 **the scratch assay** and the effect of PSAP is mimicked by TX14(A).

656 A: Astrocytes move into a wound in media containing 5% FBS and in PDM (prosaposin-
657 depleted media) supplemented with 100 nM TX14(A) but the movement is inhibited in
658 absence of PSAP. Representative images at 0, 24 and 48 hours post scratch. See also
659 supplementary movies 1-3.

660 B: Dynamics of the relative wound density under conditions shown in A (n= 3, triplicates).

661 C: Relative wound density 48 hrs post scratch for astrocytes incubated in FBS-containing
662 media, PDM, PDM +TX14(A), PDM+TX14(A)+both knock-down vectors and PDM+TX14(A)+
663 knock-down control vector n = 6, triplicates, *** P <0.001 vs. indicated group, one-way
664 ANOVA with Turkey's post-hoc analysis).

665 D: DAPI staining revealed no significant differences in the cell density between astrocytes
666 cultured in media (+FBS), PDM and PDM supplemented with TX14(A) (100 nM) (n= 15).

667 E: Addition of TX14 to PDM does not affect the numbers of new astrocytes based on BrdU
668 staining (n = 7, triplicates).

669 **Fig. 4. cAMP in astrocytes affects wound closure in the scratch assay.**

670 A: A scratch wound was created in astrocyte monolayers cultured in FBS-containing media
671 or PDM supplemented with 100 nM TX14(A). Drugs were added and dynamics of the wound
672 closure was monitored for 72 hrs (n = 5, triplicates).

673 B: DAPI staining of astrocytes shows that NKH477 (10 µM), 6-BenZ-cAMP (500 µM), and 8-
674 pCPT-2'-O-Me-cAMP (1000 µM) significantly decreased cell numbers as compared to
675 control. (n= 4, triplicates).

In both cases, one-way ANOVA with Dunnett's post-hoc analysis. ** *P* <0.01, *** *P* <0.001 vs. control.

Fig. 5. TX14(A) acts via GPR37L1 and GPR37 to protect primary astrocytes against toxicity induced by H_2O_2, staurosporine or rotenone.

A: Pre-exposure to stressors (5 hours) drastically reduce relative wound density recorded at 48 hrs in PDM. TX14(A) (100 nM) rescued astrocytes bringing wound density close to normal (compare to Fig 3). GPR37L1/GPR37 knock-down prevented the protective effect of TX14(A), while the control vector had no effect (n = 6, triplicates, *** *P* <0.001 vs. indicated group).

B: LDH release was used as a measure of cytotoxicity, 24 hrs after exposure of astrocytes to oxidative stress. In PDM manipulation of GPR37L1/GPR37 had no effect. TX14(A) (100 nM) protected them from damage but only when they were expressing GPR37L1/GPR37, (n = 6, triplicates, ** *P* <0.01, *** *P* <0.001 vs. control group, e.g. PDM groups).

One-way ANOVA with Bonferroni's post-hoc analysis.

Fig. 6. Co-cultured astrocytes protect cortical neurons against oxidative toxicity partially through GPR37L1/GPR37 signaling in astrocytes.

A: Experimental design: a - stressed neurons (blue) in absence or presence of astrocytes (green) on a culture insert; b - depletion of PSAP from the media with anti-PSAP antibodies; c - GPR37L1 and GPR37 knock-down in astrocytes co-cultured with neurons; d - GPR37L1 and GPR37 knock-down in neurons in the co-culture system.

Neurons were treated with H_2O_2 (250 μM) for 1 hr, or staurosporine (100 nM) or rotenone (50 μM) for two hrs. Stressors were then removed and inserts with astrocytes were introduced. LDH assay was carried out 24 hr later.

B: Astrocytes protect cortical neurons against H_2O_2-induced stress, the effect saturates at ~75k astrocytes per co-culture (n= 5, triplicates, *** *P* <0.001 vs. control (no astrocytes insert),**** *P* <0.0001 vs. groups with less than 50k astrocytes, one way ANOVA with Tukey's post-hoc analysis).

C: TX14(A) has a weak protective effect on neurons against oxidative stress (n = 6, triplicates, *** P <0.001, **** P <0.0001 vs 50 nM TX14(A) group (effect of 50 nM is not significant, one way ANOVA with Bonferoni's post-hoc analysis).

D: PSAP depletion or GPR37L1/GPR37 knock-down selectively in astrocytes significantly attenuates the protective effect of astrocytes on neurons pre-exposed to oxidative stressors (n = 6, triplicates, *** P <0.001 vs. indicated group, one-way ANOVA with Turkey's post-hoc analysis).

Fig. 7. Working model of the neuroprotective role of astrocytic GPR37L1/GPR37 based on the evidence presented in this study.

Damaged neurons release diffusible "SOS" factor(s) which trigger release of PSAP. PSAP acts on GPR37L1 on astrocytes and activates release of diffusible neuroprotective factor(s).

SUPPLEMENTARY FIGURES

S1. Alignment of prosaptide TX14 against PSAP of various species

S2. Expression levels of several GPR37L1, GPR37 assessed by next generation sequencing

S3. Expression levels of GPR37L1 and GPR37 in cultured and acutely isolated rat astrocytes assessed by Real Time PCR

S4. Immunodetection of PSAP contained in fetal calf serum and cell culture media

S5. GPR37L1 and GPR37 knockdown efficiency verified by Real Time PCR

S6. Astrocytes and neurons transduced with AVV-miRNA-GPR37L1/37

S7. Response of Adra 1a receptor to norepinephrine detected by Presto-TANGO system

S8. Astrocytes protect cortical neurons against oxidative stress induced by rotenone and staurosporine in a “number”-dependent manner.

S9. PSAP is produced by astrocytes and neurones.

SUPPLEMENTARY MOVIES

Supplementary Movie 1.

Wound closure dynamics in full media

Supplementary Movie 2

Wound closure dynamics in PSAP depleted media (PDM)

Supplementary Movie 3

Wound closure dynamics in PSAP depleted media supplemented with TX14(A) 100 nM

Supplementary Movie 4

Wound closure dynamics in PSAP depleted media supplemented with TX14(A) 100 nM in astrocytes where GPR37L1 and GPR37 were knocked down

Supplementary Movie 5

Wound closure dynamics in PSAP depleted media supplemented with TX14(A) 100 nM in astrocytes treated with vectors expressing control (negative) knock-down cassette

References

Anderson, MA, Burda, JE, Ren, Y, Ao, Y, O'Shea, TM, Kawaguchi, R, Coppola, G, Khakh, BS, Deming, TJ & Sofroniew, MV. (2016). Astrocyte scar formation aids central nervous system axon regeneration. *Nature*, ***532***, 195-200. DOI: 10.1038/nature17623

Bos, JL. (2003). Epac: a new cAMP target and new avenues in cAMP research. *Nat Rev Mol Cell Biol*, ***4***, 733-738. DOI: 10.1038/nrm1197

Calcutt, NA, Campana, WM, Eskeland, NL, Mohiuddin, L, Dines, KC, Mizisin, AP & O'Brien, JS. (1999). Prosaposin gene expression and the efficacy of a prosaposin-derived peptide in preventing structural and functional disorders of peripheral nerve in diabetic rats. *J Neuropathol Exp Neurol*, ***58***, 628-636.

Campana, WM, Eskeland, N, Calcutt, NA, Misasi, R, Myers, RR & O'Brien, JS. (1998). Prosaptide prevents paclitaxel neurotoxicity. *Neurotoxicology*, ***19***, 237-244.

Cantuti-Castelvetri, I, Keller-McGandy, C, Bouzou, B, Asteris, G, Clark, TW, Frosch, MP & Standaert, DG. (2007). Effects of gender on nigral gene expression and parkinson disease. *Neurobiol Dis*, ***26***, 606-614. DOI: 10.1016/j.nbd.2007.02.009

Chai, H, Diaz-Castro, B, Shigetomi, E, Monte, E, Octeau, JC, Yu, X, Cohn, W, Rajendran, PS, Vondriska, TM, Whitelegge, JP, Coppola, G & Khakh, BS. (2017). Neural Circuit-Specialized Astrocytes: Transcriptomic, Proteomic, Morphological, and Functional Evidence. *Neuron*, ***95***, 531-549. DOI: 10.1016/j.neuron.2017.06.029

Clark, RB & Perkins, JP. (1971). Regulation of adenosine 3':5'-cyclic monophosphate concentration in cultured human astrocytoma cells by catecholamines and histamine. *Proc Natl Acad Sci U S A*, ***68***, 2757-2760.

Coleman, JL, Ngo, T, Schmidt, J, Mrad, N, Liew, CK, Jones, NM, Graham, RM & Smith, NJ. (2016). Metalloprotease cleavage of the N terminus of the orphan G protein-coupled receptor GPR37L1 reduces its constitutive activity. *Sci Signal*, ***9***, ra36. DOI: 10.1126/scisignal.aad1089

Duale, H, Kasparov, S, Paton, JF & Teschemacher, AG. (2005). Differences in transductional tropism of adenoviral and lentiviral vectors in the rat brainstem. *Exp Physiol*, ***90***, 71-78. DOI: 10.1113/expphysiol.2004.029173

Dunham, JH, Meyer, RC, Garcia, EL & Hall, RA. (2009). GPR37 surface expression enhancement via N-terminal truncation or protein-protein interactions. *Biochemistry*, ***48***, 10286-10297. DOI: 10.1021/bi9013775

Gao, HL, Li, C, Nabeka, H, Shimokawa, T, Saito, S, Wang, ZY, Cao, YM & Matsuda, S. (2013). Attenuation of MPTP/MPP(+) toxicity in vivo and in vitro by an 18-mer peptide derived from prosaposin. *Neuroscience*, ***236***, 373-393. DOI: 10.1016/j.neuroscience.2013.01.007

Gao, HL, Li, C, Nabeka, H, Shimokawa, T, Wang, ZY, Cao, YM & Matsuda, S. (2016). An 18-mer Peptide Derived from Prosaposin Ameliorates the Effects of Abeta1-42 Neurotoxicity on Hippocampal Neurogenesis and Memory Deficit in Mice. *J Alzheimers Dis*, ***53***, 1173-1192. DOI: 10.3233/JAD-160093

785 Giddens, MM, Wong, JC, Schroeder, JP, Farrow, EG, Smith, BM, Owino, S, Soden, SE, Meyer, RC,
786 Saunders, C, LePichon, JB, Weinshenker, D, Escayg, A & Hall, RA. (2017). GPR37L1 modulates seizure
787 susceptibility: Evidence from mouse studies and analyses of a human GPR37L1 variant. *Neurobiol*
788 *Dis*, ***106***, 181-190. DOI: 10.1016/j.nbd.2017.07.006

789 Goldman, JE & Chiu, FC. (1984). Dibutyryl cyclic AMP causes intermediate filament accumulation and
790 actin reorganization in astrocytes. *Brain Res*, ***306***, 85-95.

791 Harenza, JL, Diamond, MA, Adams, RN, Song, MM, Davidson, HL, Hart, LS, Dent, MH, Fortina, P,
792 Reynolds, CP & Maris, JM. (2017). Transcriptomic profiling of 39 commonly-used neuroblastoma cell
793 lines. *Sci Data*, ***4***, 170033. DOI: 10.1038/sdata.2017.33

794 Hiraiwa, M, Campana, WM, Martin, BM & O'Brien, JS. (1997). Prosaposin receptor: evidence for a G-
795 protein-associated receptor. *Biochem Biophys Res Commun*, ***240***, 415-418. DOI:
796 10.1006/bbrc.1997.7673

797 Hozumi, I, Hiraiwa, M, Inuzuka, T, Yoneoka, Y, Akiyama, K, Tanaka, R, Kikugawa, K, Nakano, R, Tsuji, S
798 & O'Brien, JS. (1999). Administration of prosaposin ameliorates spatial learning disturbance and
799 reduces cavity formation following stab wounds in rat brain. *Neurosci Lett*, ***267***, 73-76.

800 Imai, Y, Soda, M, Inoue, H, Hattori, N, Mizuno, Y & Takahashi, R. (2001). An unfolded putative
801 transmembrane polypeptide, which can lead to endoplasmic reticulum stress, is a substrate of
802 Parkin. *Cell*, ***105***, 891-902.

803 Jolivalt, CG, Dacunha, JM, Esch, FS & Calcutt, NA. (2008). Central action of prosaptide TX14(A)
804 against gp120-induced allodynia in rats. *Eur J Pain*, ***12***, 76-81. DOI: 0.1016/j.ejpain.2007.03.008

805 Jolivalt, CG, Ramos, KM, Herbetsson, K, Esch, FS & Calcutt, NA. (2006). Therapeutic efficacy of
806 prosaposin-derived peptide on different models of allodynia. *Pain*, ***121***, 14-21. DOI:
807 10.1016/j.pain.2005.11.013

808 Jolly, S, Bazargani, N, Quiroga, AC, Pringle, NP, Attwell, D, Richardson, WD & Li, H. (2017). G protein-
809 coupled receptor 37-like 1 modulates astrocyte glutamate transporters and neuronal NMDA
810 receptors and is neuroprotective in ischemia. *Glia*, ***66***, 47-61. DOI: 10.1002/glia.23198

811 Kishimoto, Y, Hiraiwa, M & O'Brien, JS. (1992). Saposins: structure, function, distribution, and
812 molecular genetics. *J Lipid Res*, ***33***, 1255-1267.

813 Klarenbeek, J, Goedhart, J, van, BA, Groenewald, D & Jalink, K. (2015). Fourth-generation epac-based
814 FRET sensors for cAMP feature exceptional brightness, photostability and dynamic range:
815 characterization of dedicated sensors for FLIM, for ratiometry and with high affinity. *PLoS ONE*, ***10***,
816 e0122513. DOI: 10.1371/journal.pone.0122513

817 Klarenbeek, J & Jalink, K. (2014). Detecting cAMP with an EPAC-based FRET sensor in single living
818 cells. *Methods Mol Biol*, ***1071***, 49-58. DOI: 10.1007/978-1-62703-622-1_4

819 Kotani, Y, Matsuda, S, Sakanaka, M, Kondoh, K, Ueno, S & Sano, A. (1996a). Prosaposin facilitates
820 sciatic nerve regeneration in vivo. *J Neurochem*, ***66***, 2019-2025.

821 Kotani, Y, Matsuda, S, Wen, TC, Sakanaka, M, Tanaka, J, Maeda, N, Kondoh, K, Ueno, S & Sano, A.
822 (1996b). A hydrophilic peptide comprising 18 amino acid residues of the prosaposin sequence has
823 neurotrophic activity in vitro and in vivo. *J Neurochem*, ***66***, 2197-2200.

Kroeze, WK, Sassano, MF, Huang, XP, Lansu, K, McCorvy, JD, Giguere, PM, Sciaky, N & Roth, BL. (2015). PRESTO-Tango as an open-source resource for interrogation of the druggable human GPCRome. *Nat Struct Mol Biol*, ***22***, 362-369. DOI: 10.1038/nsmb.3014

Lalo, U & Pankratov, Y. (2017). Exploring the Ca(2+)-dependent synaptic dynamics in vibro-dissociated cells. *Cell Calcium*, ***64***, 91-101. DOI: 10.1016/j.ceca.2017.01.008

Leng, N, Gu, G, Simerly, RB & Spindel, ER. (1999). Molecular cloning and characterization of two putative G protein-coupled receptors which are highly expressed in the central nervous system. *Brain Res Mol Brain Res*, ***69***, 73-83.

Liu, B, Teschemacher, AG & Kasparov, S. (2017). Astroglia as a cellular target for neuroprotection and treatment of neuro-psychiatric disorders. *Glia*, ***65***, 1205-1226. DOI: 10.1002/glia.23136

Liu, B, Xu, H, Paton, JF & Kasparov, S. (2010). Cell- and region-specific miR30-based gene knock-down with temporal control in the rat brain. *BMC Mol Biol*, ***11***, 93. DOI: 10.1186/1471-2199-11-93

Lu, AG, Otero, DA, Hiraiwa, M & O'Brien, JS. (2000). Neuroprotective effect of retro-inverso Prosaptide D5 on focal cerebral ischemia in rat. *NeuroReport*, ***11***, 1791-1794.

Marazziti, D, Mandillo, S, Di, PC, Golini, E, Matteoni, R & Tocchini-Valentini, GP. (2007). GPR37 associates with the dopamine transporter to modulate dopamine uptake and behavioral responses to dopaminergic drugs. *Proc Natl Acad Sci U S A*, ***104***, 9846-9851. DOI: 10.1073/pnas.0703368104

Mattila, SO, Tuusa, JT & Petaja-Repo, UE. (2016). The Parkinson's-disease-associated receptor GPR37 undergoes metalloproteinase-mediated N-terminal cleavage and ectodomain shedding. *J Cell Sci*, ***129***, 1366-1377. DOI: 10.1242/jcs.176115

Meyer, RC, Giddens, MM, Schaefer, SA & Hall, RA. (2013). GPR37 and GPR37L1 are receptors for the neuroprotective and glioprotective factors prosaptide and prosaposin. *Proc Natl Acad Sci U S A*, ***110***, 9529-9534. DOI: 10.1073/pnas.1219004110

Ngo, T, Ilatovskiy, AV, Stewart, AG, Coleman, JL, McRobb, FM, Riek, RP, Graham, RM, Abagyan, R, Kufareva, I & Smith, NJ. (2017). Orphan receptor ligand discovery by pickpocketing pharmacological neighbors. *Nat Chem Biol*, ***13***, 235-242. DOI: 10.1038/nchembio.2266

O'Brien, JS, Carson, GS, Seo, HC, Hiraiwa, M & Kishimoto, Y. (1994). Identification of prosaposin as a neurotrophic factor. *Proc Natl Acad Sci U S A*, ***91***, 9593-9596.

Otero, DA, Conrad, B & O'Brien, JS. (1999). Reversal of thermal hyperalgesia in a rat partial sciatic nerve ligation model by Prosaptide TX14(A). *Neurosci Lett*, ***270***, 29-32.

Sano, A, Matsuda, S, Wen, TC, Kotani, Y, Kondoh, K, Ueno, S, Kakimoto, Y, Yoshimura, H & Sakanaka, M. (1994). Protection by prosaposin against ischemia-induced learning disability and neuronal loss. *Biochem Biophys Res Commun*, ***204***, 994-1000. DOI: 10.1006/bbrc.1994.2558

Smith, NJ. (2015). Drug Discovery Opportunities at the Endothelin B Receptor-Related Orphan G Protein-Coupled Receptors, GPR37 and GPR37L1. *Front Pharmacol*, ***6***, 275. DOI: 10.3389/fphar.2015.00275

Southern, C, Cook, JM, Neetoo-Isseljee, Z, Taylor, DL, Kettleborough, CA, Merritt, A, Bassoni, DL, Raab, WJ, Quinn, E, Wehrman, TS, Davenport, AP, Brown, AJ, Green, A, Wigglesworth, MJ & Rees, S.

(2013). Screening beta-Arrestin Recruitment for the Identification of Natural Ligands for Orphan G-Protein-Coupled Receptors. *J Biomol Screen*, ***18***, 599-609. DOI: 10.1177/1087057113475480

Sun, Y, Qi, X, Witte, DP, Ponce, E, Kondoh, K, Quinn, B & Grabowski, GA. (2002). Prosaposin: threshold rescue and analysis of the "neuritogenic" region in transgenic mice. *Mol Genet Metab*, ***76***, 271-286.

Tardy, M, Fages, C, Rolland, B, Bardakdjian, J & Gonnard, P. (1981). Effect of prostaglandins and dibutyryl cyclic AMP on the morphology of cells in primary astroglial cultures and on metabolic enzymes of GABA and glutamate metabolism. *Experientia*, ***37***, 19-21.

Yan, L, Otero, DA, Hiraiwa, M & O'Brien, JS. (2000). Prosaptide D5 reverses hyperalgesia: inhibition of calcium channels through a pertussis toxin-sensitive G-protein mechanism in the rat. *Neurosci Lett*, ***278***, 120-122.

Zhang, Y, Chen, K, Sloan, SA, Bennett, ML, Scholze, AR, O'Keeffe, S, Phatnani, HP, Guarnieri, P, Caneda, C, Ruderisch, N, Deng, S, Liddelow, SA, Zhang, C, Daneman, R, Maniatis, T, Barres, BA & Wu, JQ. (2014). An RNA-Sequencing Transcriptome and Splicing Database of Glia, Neurons, and Vascular Cells of the Cerebral Cortex. *J Neurosci*, ***34***, 11929-11947. DOI: 10.1073/pnas.1219004110

Zhang, Y, Sloan, SA, Clarke, LE, Caneda, C, Plaza, CA, Blumenthal, PD, Vogel, H, Steinberg, GK, Edwards, MS, Li, G, Duncan, JA, III, Cheshier, SH, Shuer, LM, Chang, EF, Grant, GA, Gephart, MG & Barres, BA. (2016). Purification and Characterization of Progenitor and Mature Human Astrocytes Reveals Transcriptional and Functional Differences with Mouse. *Neuron*, ***89***, 37-53. DOI: 10.1016/j.neuron.2015.11.013

Fig 1

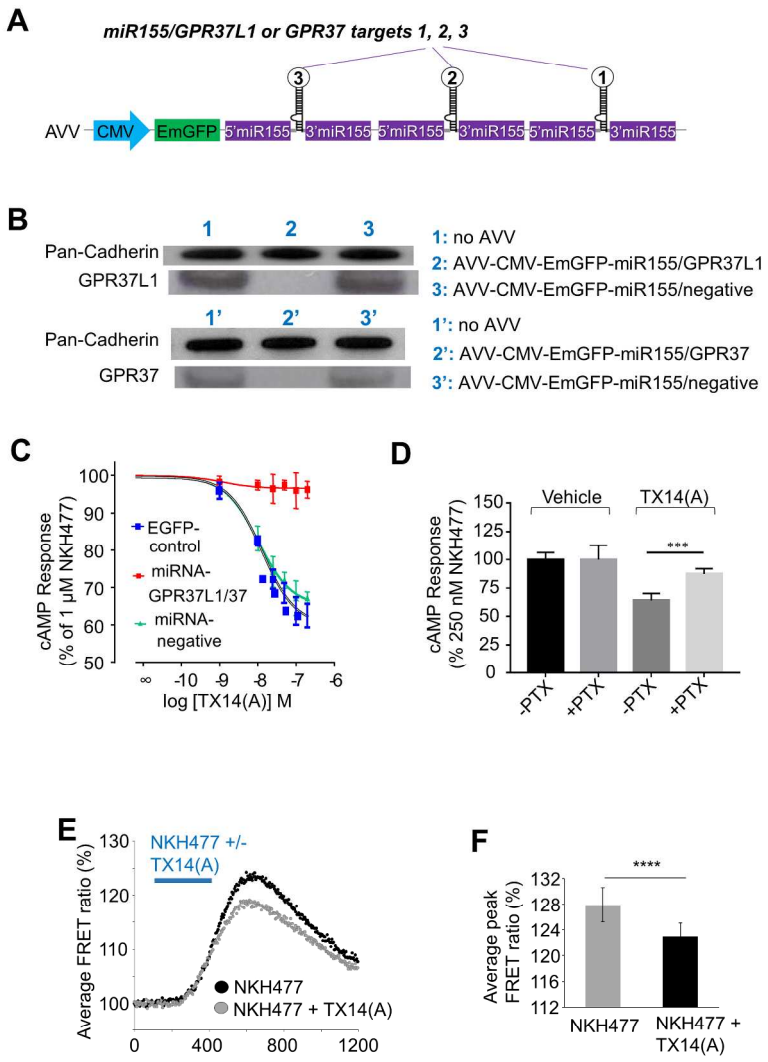

Figure 1

190x275mm (300 x 300 DPI)

Fig 2

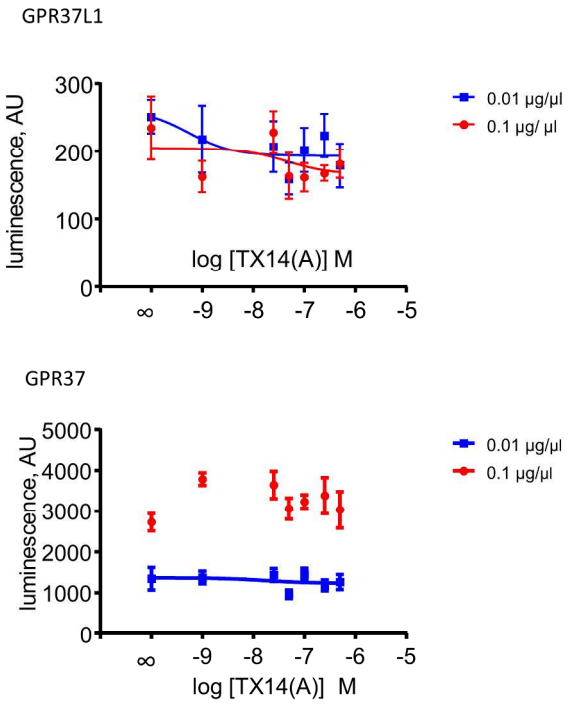

Figure 2

190x275mm (300 x 300 DPI)

Fig 3

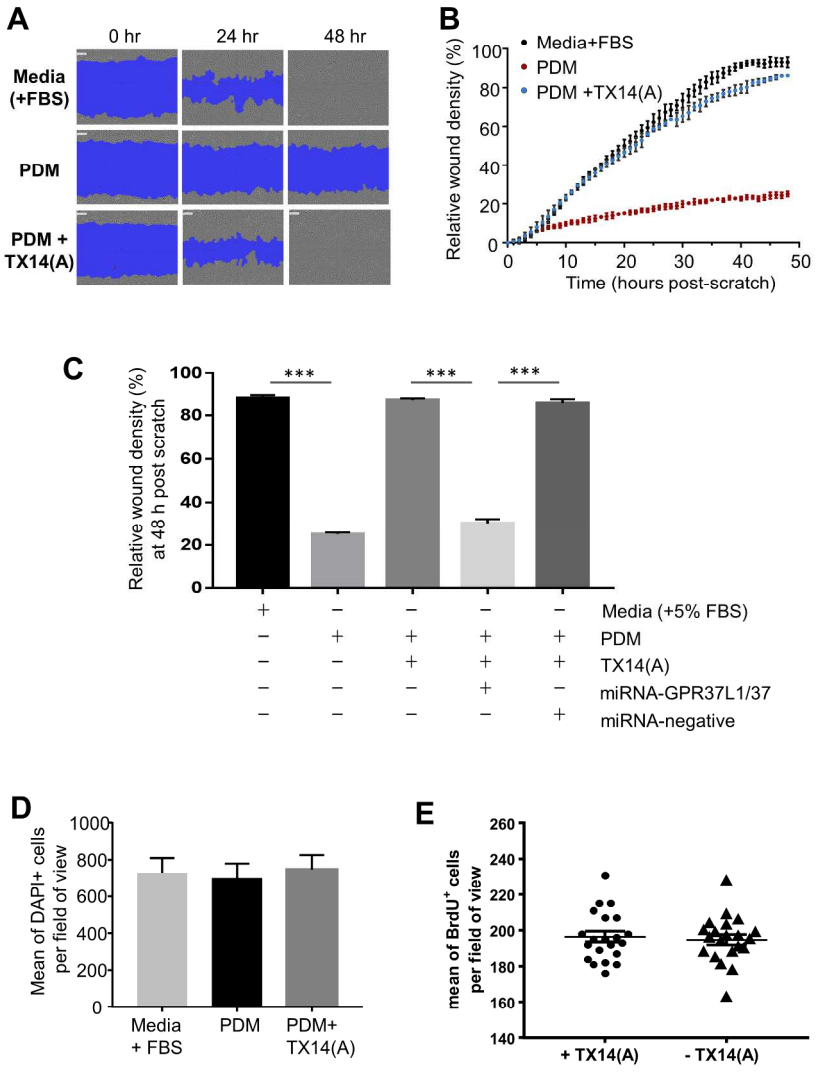

Figure 3

190x275mm (300 x 300 DPI)

Fig 4

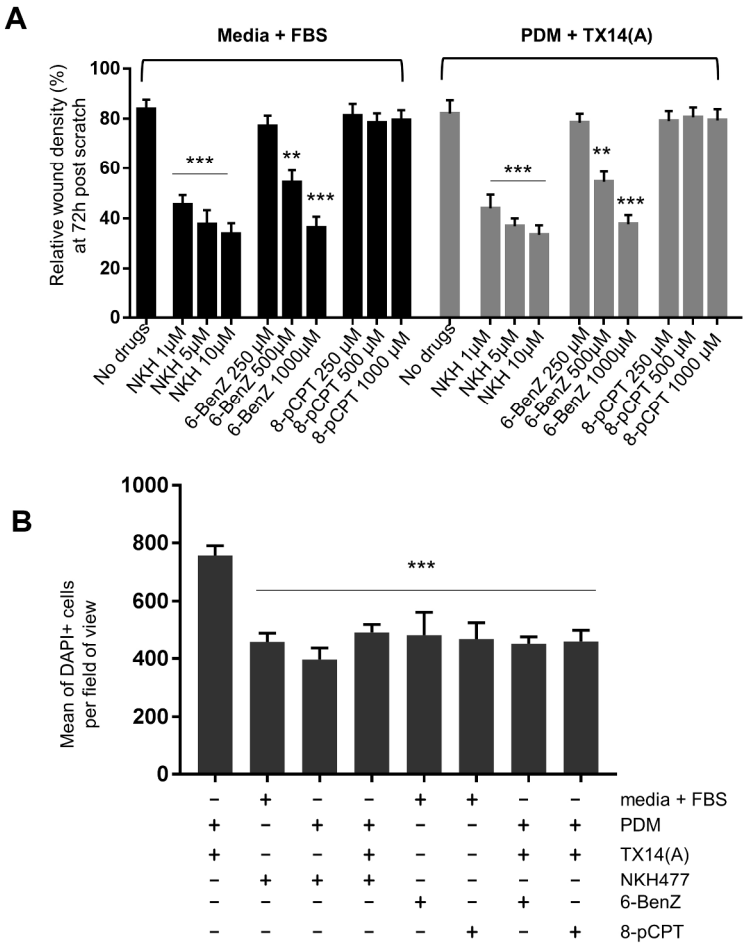

Figure 4

190x275mm (300 x 300 DPI)

Fig 5

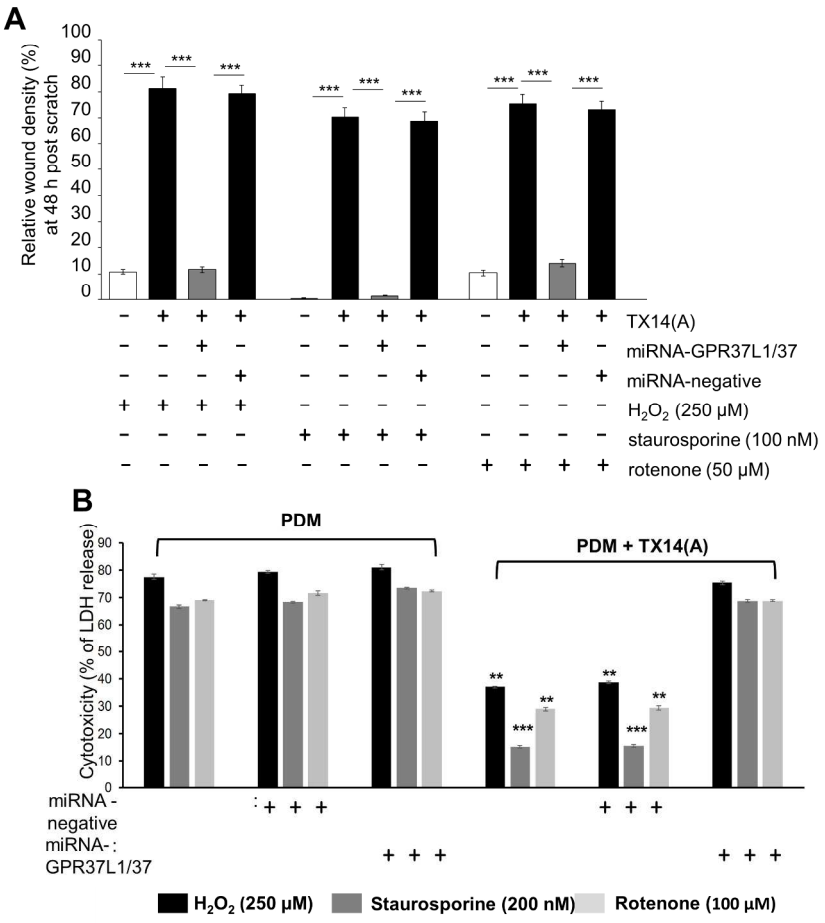

Figure 5

190x275mm (300 x 300 DPI)

Fig 6

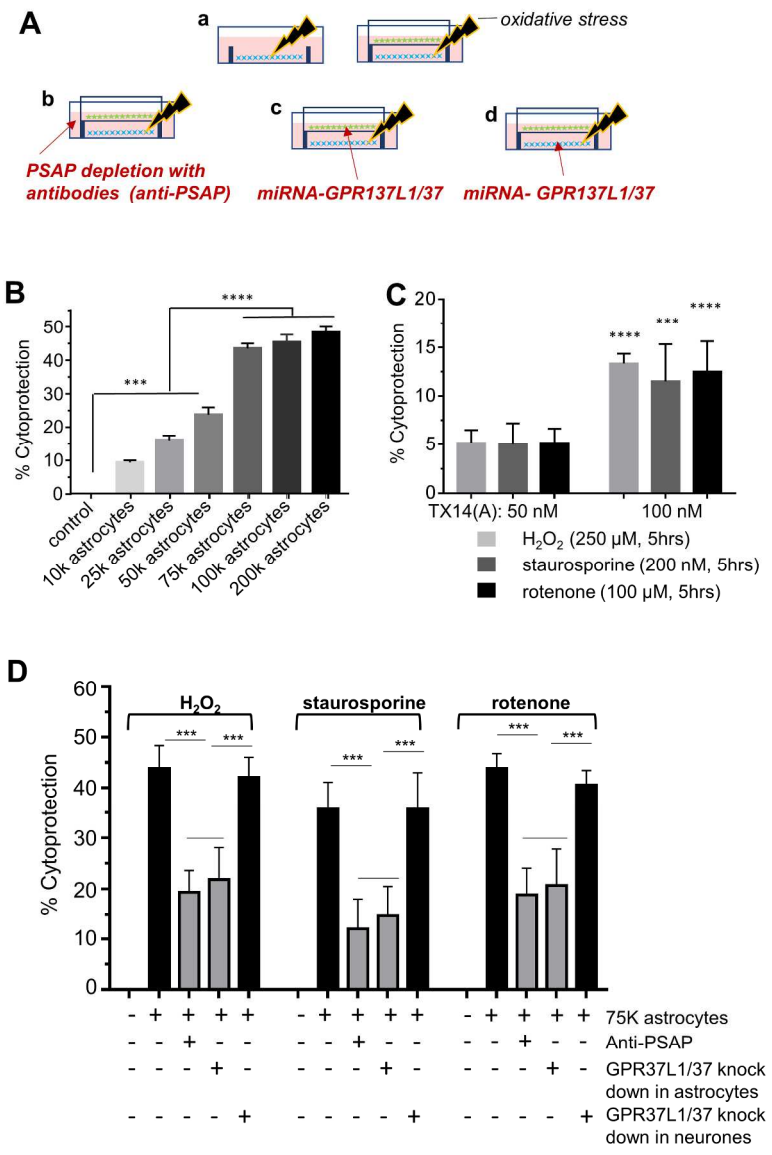

Figure 6

190x275mm (300 x 300 DPI)

Fig 7

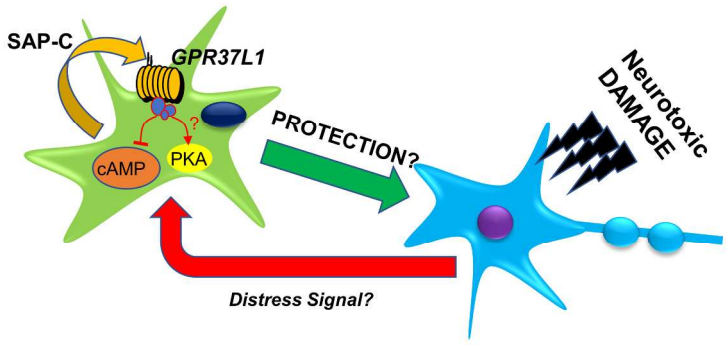

Figure 7

190x275mm (300 x 300 DPI)

S1

prosaptideTX	T	A	L	I	D	N	N	A	T	E		E	I	I	Y
SAP_HUMAN	T	K	L	I	D	N	N	K	T	E	K	E	I	L	
SAP_MOUSE	S	E	L	I	V	N	N	A	T	E	E	L	L	V	K
SAP_BOVIN	A	K	L	I	D	N	N	R	T	E	E	E	I	L	H
SAP_RAT	S	E	L	I	I	N	N	A	T	E	E	L	L	I	K
SAP_CAVPO	M	E	L	I	D	N	N	R	T	E	E	K	I	I	H

Alignment of prosaptide TX14 against PSAP of various species shows that the signalling sequence is highly conserved. Image below – a computer model of SAP-C in the closed conformation (Protein Data Bank) where the TX14 sequence is looking outwards in the hinge region.

Supplementary Figure 1

190x275mm (300 x 300 DPI)

S2

RECEPTOR	Brainstem P3	Brainstem Adult	Cortex P3	Cortex Adult
GPR37	5	112	2	1.4
GPR37L1	73	115	25	5
P2Y1R	0.2	1	0.6	11
PAR-1	26	27	35	17

Expression levels of several GPR37L1, GPR37 and two other representative for astrocytes G-protein coupled receptors as assessed by NGS. Rat astrocytes were isolated (FACS sorting with GLAST antibodies). Values are FPKM (duplicates). P2Y1R and PAR-1 receptors are listed for reference as two G-protein coupled receptors commonly implicated in astrocyte biology.

For reference:

1. In the Stanford databases (Zhang et al datasets, (Zhang et al., 2016;Zhang et al., 2014), GPR37 is above noise in astrocytes in both human and mouse (~3-5 FPKM), while for the GPR37L1 the human reads are at ~ 60 FPKM and for mouse at ~370 (e.g. ~100 fold difference). This, suggests that there is a significant difference in the dominance of GPR37L1 between the two species.
2. In the transcriptome of spinal cord astrocytes level of GPR37L1 is roughly 10 times greater than that of GPR37, not taking into account issues related to the use of FPKM as a measure of relative expression. (Anderson et al., 2016)
https://astrocyte.rnaseq.sofroniewlab.neurobio.ucla.edu
3. In UCLA database (Chai et al., 2017) which is based on a TRAP approach in cortical, striatal and hippocampal astrocytes, FPKM for GPR37L1 are 700-100 times higher than for GPR37. It seems that in the cortex GPR37L1 is by far the most dominant but in deeper structures difference is much less pronounced.
http://astrocyternaseq.org/
http://astrocyternaseq.org/addgene?query=Gpr37l1
http://astrocyternaseq.org/addgene?query=Gpr37
4. In a database of transcriptomes of neuroblastomas, where human fetal astrocytes are also listed, GPR37 is expressed in astrocytes at a level only lightly lower than that of ADRA2A – one of the best documented Gi coupled GPCR on astrocytes (Harenza et al., 2017).

Supplementary Figure 2

190x275mm (300 x 300 DPI)

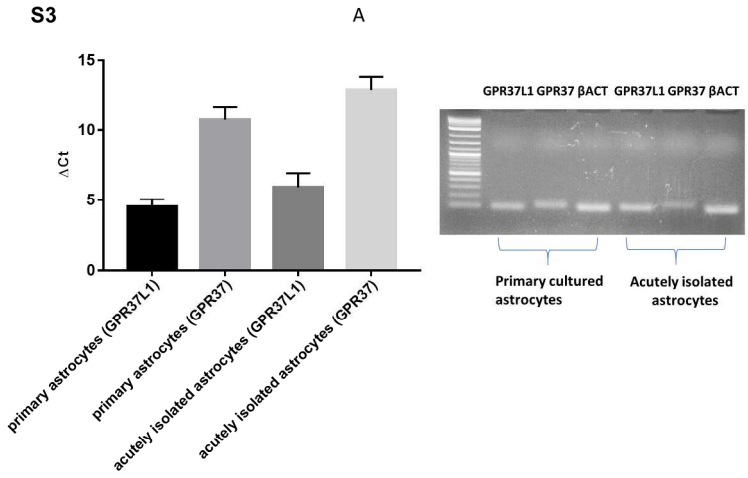

GPR37 and GPR37L1 are expressed by primary cultured and acutely isolated astrocytes.
In order to verify that the expression of GPR37L1 and GPR37 in our cultured astrocytes is not an result of culturing, we performed vibro-isolation of cortical astrocytes from P12 Wistar rats using a method recently described by Lalo and Pankratov (Cell Calcium, 2017, 64, 91-101). ~50 single astrocytes were manually collected from the bottom of a small Petri dish into a sterile test tube. Ambion Power SYBR Green Cells to Ct kit was used to directly generate cDNA. cDNA was then used for Real Time PCR. Note that higher ΔCt vs β-actin is an indication of lower level of expression of GPR37 than of GPR37L1.

Left: The difference between the cycle thresholds (ΔCT) of GPR37L1 and GPR37 against a reference housekeeping gene β-actin.

Right: Agarose gel demonstrating Real Time RT-PCR products for ß-actin, GPR37L1 and GPR37. Expected product sizes: ß-actin 98 BP, GPR37L1 96BP and GPR37 114 bp. Left: 2-log ladder, the lower band: 100 bp.

Supplementary Figure 3

190x275mm (300 x 300 DPI)

S4

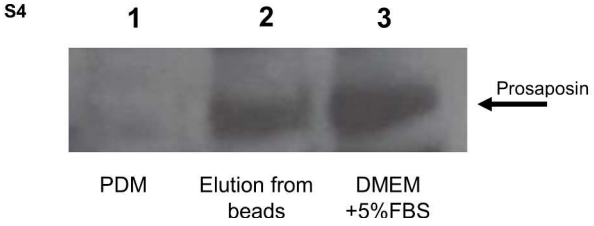

PSAP contained in fetal calf serum and cell culture media can be depleted by using anti-PSAP antibody and Protein A Magnetic Beads as demonstrated by Western blot of PSAP.
Lane 1 - prosaposin-depleted media
Lane 2 – Prosaposin was adsorbed to and removed with PSAP-antibody conjugated magnetic beads.
Lane 3 – PSAP in the regular serum-supplemented culture media.

Supplementary Figure 4

190x275mm (300 x 300 DPI)

S5

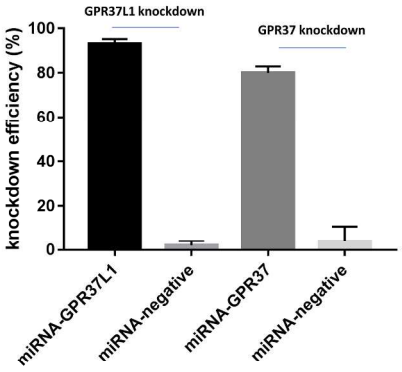

GPR37L1 and GPR37 knockdown efficiency measured by Real Time PCR. Primary cultured rat astrocytes were seeded in 24 well plates at 1X10^5 per well. They were transduced with AVV-CMV-EmGFP-miR155/GPR37L1, AVV-CMV-EmGFP-miR155/GPR37 or AVV-CMV-EmGFP-miR155/negative at MOI 10. Two days later, total RNA were extracted from the cells and two step RT-PCR was carried out. Knockdown efficiency was calculated as: $(1\text{-}2^{\wedge\Delta(\text{Ct no virus-}\Delta\text{CtmiRNA-GPR3L1 or GPR37})}*100\%$ where ΔCt no virus $=(Ct_{\text{GPR37L1 or GPR37}} - Ct_{\text{ß-actin}})$ of the control sample and $\Delta Ct_{\text{miRNA-GPR37L1 or GPR37}} = (Ct_{\text{GPR37L1 or GPR37}} - Ct_{\text{ß-actin}})$ of the transduced samples.

Supplementary Figure 5

190x275mm (300 x 300 DPI)

S6

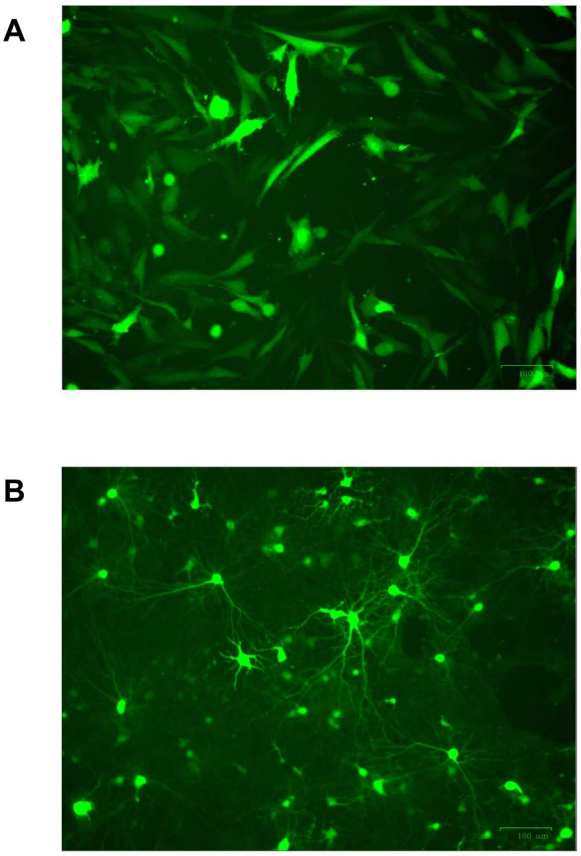

Astrocytes and neurons transduced with AVV-miRNA-GPR37L1/37 (mixture of AVV-CMV-EmGFP-miR155/GPR37L1 and AVV-CMV-EmGFP-miR155/GPR37) are healthy and express the fluorescent marker EmGFP. A: astrocytes B: cortical neurons.

Supplementary Figure 6

190x275mm (300 x 300 DPI)

S7

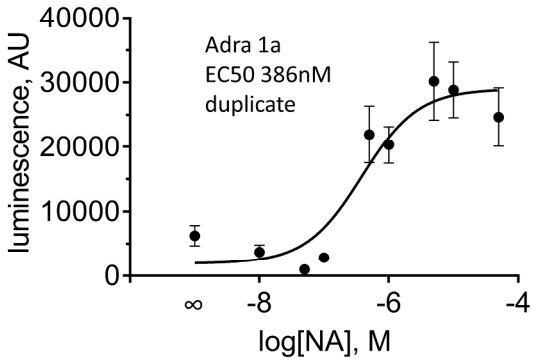

Response of Adra 1a receptor to norepinephrine detected by Presto-TANGO system (Kroeze et al 2015). In this assay agonist-induced recruitment of β-arrestin leads to expression of luciferase which is detected as a measure of receptor activation.

Supplementary Figure 7

190x275mm (300 x 300 DPI)

S8

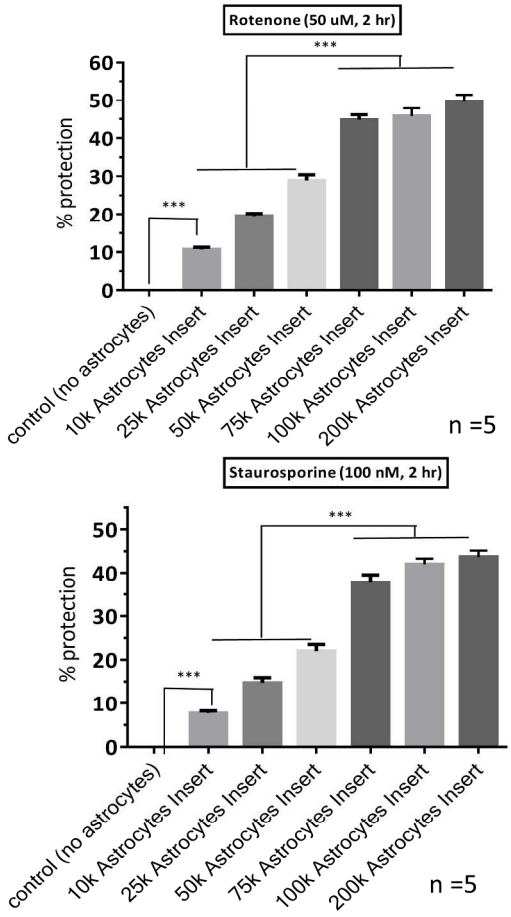

Astrocytes protect cortical neurons against oxidative stress induced by rotenone and staurosporine in a "number"-dependent manner.

Supplementary Figure 8

190x275mm (300 x 300 DPI)

S9

PSAP is produced by astrocytes and neurones. When astrocytes are placed together with the stressed neurones, this triggers a surge of PSAP in the media, although the cellular origin of PSAP in this experiment is unknown

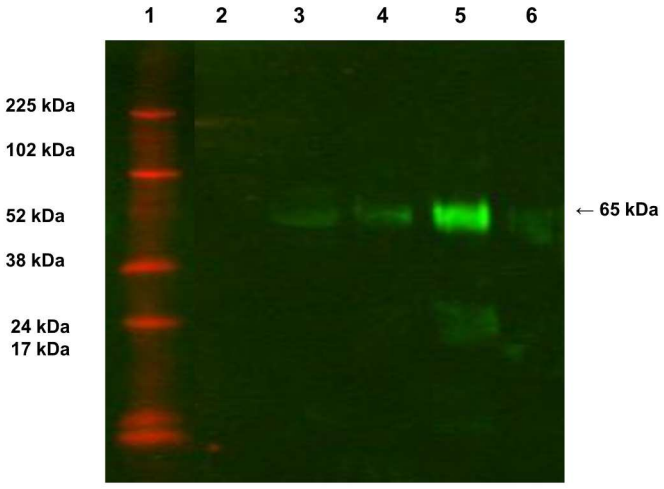

1: ECL plex fluorescent rainbow markers
2: unconcentrated media from H_2O_2-treated cortical neurons
3: PSAP Human Recombinant standard, 200 ng
4: 1000 x concentrated media from H_2O_2-treated cortical neurons
5: 1000 x concentrated media from astrocytes/cortical neurons (H_2O_2-treated) co-culture
6: 1000 x concentrated media from astrocytes only culture

Western blot evidence of the existence of PSAP from co-culture media when neurons are exposed to 250 uM H2O2. Lane 1: ECL plex fluorescent rainbow markers. Lane 2: unconcentrated media from H2O2-treated cortical neurons. 3: PSAP Recombinant standard, 200 ng. 4: 1000 x concentrated media from H2O2-treated cortical neurons. 5: 1000 x concentrated media from co-culture where neurons are treated with H2O2-treated. 6: 1000 x concentrated media from unstressed astrocytes only culture. Media were concentrated by sequentially using Amicon Ultra centrifugal filter units (Ultra-15, MWCO 30 kDa), Amicon Ultra centrifugal filter units (Ultra-4, MWCO 30 kDa) and Microcon-10kDa Centrifugal Filter Unit (Millipore).

Supplementary Figure 9

190x275mm (300 x 300 DPI)

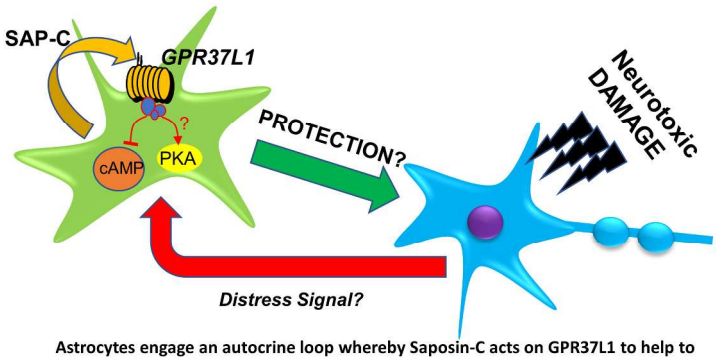

Astrocytes engage an autocrine loop whereby Saposin-C acts on GPR37L1 to help to rescue neurones, affected by oxidative stress

TOCI

190x275mm (300 x 300 DPI)